

Article

A Preliminary Study Was Conducted on the Compressive Strength and Flow Performance of Environmentally Friendly UHPC-SCA

Shuwei Wang ^{1,2,3,4}, Min Zhang ¹, Yaoyang Shi ², Lixin Chen ² and Yingming Zhou ^{2,*} 

¹ School of Civil Engineering, Guangxi University, Nanning 530004, China; wangshuwei@bbgu.edu.cn (S.W.); 2110391153@st.gxu.edu.cn (M.Z.)

² College of Architecture and Engineering, Beibu Gulf University, Qinzhou 535011, China; syy2015402132@yeah.net (Y.S.); clx2015402201@yeah.net (L.C.)

³ Guangxi Key Laboratory of Ocean Engineering Equipment and Technology, Qinzhou 535011, China

⁴ Key Laboratory of Beibu Gulf Offshore Engineering Equipment and Technology (Beibu Gulf University), Education Department of Guangxi Zhuang Autonomous Region, Qinzhou 535011, China

* Correspondence: zhouyingming@bbgu.edu.cn; Tel.: +86-17877278558

Abstract: This research paper explores using marine shells as coarse aggregates in producing seawater sea sand UHPC-CA. The study examined factors such as coarse aggregates (granite, oyster shell, and cone shell), fine aggregates (sea sand and river sand), fiber types, and content. The research findings indicate that different coarse aggregates and fibers influence the flow performance of UHPC-SCA. The study identified the cone shell as the best coarse shell aggregate and 1.5% steel fiber as the optimal fiber and inclusion amount. The compressive strength of this combination reached 106 MPa, which is comparable to the granite stone UHPC-CA of the same particle size.

Keywords: marine shell; UHPC-SCA; fluidity; compressive strength



Citation: Wang, S.; Zhang, M.; Shi, Y.; Chen, L.; Zhou, Y. A Preliminary Study Was Conducted on the Compressive Strength and Flow Performance of Environmentally Friendly UHPC-SCA. *Buildings* **2023**, *13*, 2226. <https://doi.org/10.3390/buildings13092226>

Academic Editors: Yanni Bouras, Le Li and Wasantha Liyanage

Received: 24 July 2023

Revised: 25 August 2023

Accepted: 29 August 2023

Published: 31 August 2023



Copyright: © 2023 by the authors. Licensee MDPI, Basel, Switzerland. This article is an open access article distributed under the terms and conditions of the Creative Commons Attribution (CC BY) license (<https://creativecommons.org/licenses/by/4.0/>).

1. Introduction

The demand for concrete performance in engineering is increasing with the rapid development of the social economy and infrastructure construction. In 1994, experts from different countries researched and created ultra-high-performance concrete (UHPC) [1]. According to the study, UHPC has better compression resistance, toughness, durability, and wear resistance than regular concrete [2]. Nevertheless, UHPC has its drawbacks, mainly its significant usage of cementing material and high cost. To enhance UHPC, scholars have introduced coarse aggregate to create ultra-high-performance concrete with coarse aggregate (UHPC-CA) [3]. Incorporating fibers into the concrete mixture reduced the amount of cementing material used. This increased the bonding force between the reinforced concrete and created an anchoring effect between the aggregate and fiber. Furthermore, the occlusal product between the aggregate was improved. These results were cited in reference [4]. Liu et al. [5] created UHPC with a coarse aggregate with a maximum particle size of 5 mm. They discovered that the tensile properties of the UHPC remained unchanged if the crude aggregate content was less than 25%. According to the study by Kim et al. [6], the perfect blend for ultra-high-performance concrete involves a combination of aggregates with different particle sizes that result in the concrete's highest self-fluidity and lowest plastic viscosity. This mixture leads to a compressive strength of over 190 MPa. According to research by Shao Huli [7], the power of ultra-high-performance concrete containing basalt aggregate (UHPC-CA) largely relies on the micromechanical properties of the coarse aggregate, ITZ, and matrix. In his research, Peng Gaifei [8] examined the various factors that affect the compressive strength of UHPC-CA. These factors included the water–binder ratio, the particle size of coarse aggregate, the fineness modulus of fine aggregate, the content of cementing material, mineral admixture, and steel fiber. Gaifei found that a water–binder

ratio of 0.18 and a mass ratio of silica fume, fly ash, and mineral powder at 1:2:1 was the most effective way to improve the compressive strength of UHPC-CA. A study by Yuan Huang [9] examined the bonding performance between UHPC and steel bars through the pull-out test of UHPC-CA. The study analyzed the impact of various factors such as aggregate strength, size, content, fiber content, cover thickness, and bond length. The findings indicated that adding coarse aggregate can prevent the spread of microcracks. Additionally, increasing the range of coarse aggregate from 0 to 600 kg/m³ can lead to a 15% increase in bond strength, with the coarse aggregate of particle size 5–8 mm being the most effective at enhancing bond strength compared to other measures. In a study conducted by Huang Zhengyu et al. [10], they examined the mechanical properties of UHPC-CA and how they relate to the content of coarse aggregate and steel fiber. Their findings showed that the compressive strength of UHPC initially increases and then decreases as the content of coarse aggregate increases from 0–800 kg/m³. Meanwhile, the static compression and elastic modulus have a near-linear increase. However, when the content of coarse aggregate ranges from 0–400 kg/m³, the fluidity, flexural tensile strength, and initial cracking strength of UHPC remain relatively consistent. But when the crude aggregate content is increased to 400~800 kg/m³, these three properties of UHPC significantly decrease. In a study conducted by Fengling Yang et al. [11], it was discovered that adding coarse aggregate to ultra-high-performance concrete greatly impacted its slump. As the rough aggregate amount increased, the fresh UHPC slump decreased. However, at a content level of 20%, the fluidity of UHPC remained good while its compressive strength peaked. Zhang Xiao [12] conducted a study on the effects of particle size and coarse aggregate content on the performance of UHPC. It was discovered that as the scope and particle size of the coarse aggregate increased, the working version of UHPC decreased. However, the compressive strength of UHPC was the highest when 5–10 mm, 5–16 mm, and 5–20 mm coarse aggregates were added, with values of 15%, 15%, and 10%, respectively. Adding coarse aggregate to UHPC is a promising trend for the future because it does not compromise strength and shrinkage, has excellent lightweight characteristics, and is suitable for prestressed concrete structures [13].

Marine shells are valuable resources with many applications, including seawalls, coastlines, island reef construction, and marine structures. It is essential to adopt a sustainable approach to utilizing these shells to address the issue of shell waste and the scarcity of natural aggregate in China [14]. Many experts have researched the potential of marine shells in the construction industry. Carolina Martínez-García [15] experimented with using mussels as coarse aggregate for making concrete and found that the replacement of traditional fine or coarse aggregate with mussels should not exceed 25%. Moreover, the replacement should not exceed 12.5% of the ordinary coarse and fine aggregate used. In a study by Khankhaje [16], crushed scallop shell powder was separated into 6.30 mm and 4.75 mm and tested as a replacement for limestone at 0%, 20%, 50%, and 75%. The results showed that while using crushed scallop shells as a substitute for natural aggregate does reduce compressive strength, the range of compressive strength for permeable concrete is still acceptable after 28 days. In another experiment by Zheng Xiumei [17], six kinds of mortar with different snail replacement rates were used to replace river sand; with the increase in snail replacement rate, mortar specimens' compressive strength and flexural strength improved significantly at all ages. This was due to the unique surface state of cone snail, a reasonable admixture, and better particle gradation. A study on the seashell concrete design prediction model by Alidoust [18] successfully predicted the mechanical properties. The study suggests incorporating many seashells into the concrete mixture may reduce strength. However, using a small quantity of seashells will not significantly affect the strength parameters. Meanwhile, Poliana Bellei [19] systematically classified the scientific achievements of oyster shell composites in architecture. Bellei used the Scopus tool to search and made a detailed summary according to PRISMA. The results indicate that adding oyster shells to a cement mortar has excellent application prospects.

To summarize, marine shells are not commonly utilized in UHPC. However, numerous discarded shells are in the experimental area depicted in Figure 1 of this paper. If these shells are not repurposed, they must be disposed of by dumping or burying them in place [20]. This study involved researchers developing ultra-high-performance concrete (UHPC-SCA) using shell coarse aggregate sea sand. They incorporated 500 kg/m³ of waste shell, 1.5–2% fiber dosage [21], and a water–binder ratio of 0.16. The team then assessed the concrete’s fluidity and compressive strength. Utilizing local materials for coastal construction has the potential to save costs and reduce cycle time. Furthermore, this concrete can enhance structures and provide crucial safety measures for marine development.



Figure 1. Waste shells.

2. Experimental Preparation

2.1. Experimental Materials

The experiment is in Qinzhou City’s Qinnan District, Guangxi, at Beibu Gulf University. The area has abundant marine resources, particularly oysters, corals, and snails.

2.1.1. Coarse Aggregate

For this experiment, we used coarse aggregate from oyster shells and cone shells, which we collected from the seaside. We cleaned, dried, crushed, and screened the aggregate. Table 1 displays its fundamental performance compared to granite gravel with the same particle size.

Table 1. The physical properties of various coarse aggregates.

| Category | Particle Size (mm) | Apparent Density (kg/m ³) | Bulk Density (kg/m ³) | Porosity (%) | Mud Content (%) | Water Content (%) |
|---------------|--------------------|---------------------------------------|-----------------------------------|--------------|-----------------|-------------------|
| Granite | 4.75–9.50 | 2671 | 1425 | 46.45 | 1.52 | 1.24 |
| Oyster shells | 4.75–9.50 | 2357.6 | 942.1 | 60.00 | 0.17 | 12.13 |
| Cone shells | 4.75–9.50 | 2765 | 1223 | 55.77 | 0.13 | 2.56 |

2.1.2. Fine Aggregate

There are two types of experimental fine aggregate: sea sand collected from Sanniang Bay, Qinzhou, Guangxi and river sand from a typical sand mining field. Table 2 presents the physical properties of both acceptable aggregate types.

Table 2. Physical properties of fine aggregate.

| Category | Particle Size (mm) | Apparent Density (kg/m ³) | Bulk Density (kg/m ³) | Porosity (%) | Mud Content (%) | Water Content (%) |
|------------|--------------------|---------------------------------------|-----------------------------------|--------------|-----------------|-------------------|
| River Sand | 2.72 | 2647 | 1725 | 34.84 | 3.4 | 0.14 |
| Sea sand | 2.66 | 2667 | 1480 | 44.51 | 0.4 | 0.82 |

2.1.3. Mixing Water

The water mixture is separated into regular tap water and seawater from the nearby Sanniangwan Ocean Observatory. China Guangxi Autonomous Region Qinzhou Hengqin Testing Technology Co., Ltd. analyzed the composition and content of the water, as indicated in Table 3.

Table 3. Seawater test results in Sanniang Bay.

| Detection Component | Cl ⁻ /Mg/L | SO ₄ ²⁻ /Mg/L | Na ⁺ /Mg/L | Ca ²⁺ /Mg/L | Mg ²⁺ /Mg/L |
|---------------------|------------------------|-------------------------------------|------------------------|------------------------|------------------------|
| Testing result | 2.06 × 10 ⁴ | 2.08 × 10 ³ | 1.38 × 10 ⁴ | 330 | 1.33 × 10 ³ |

2.1.4. Cement

For the experiment, we utilized the Conch brand of ordinary Portland cement with a grade of P·O42.5. This particular cement was produced in Fusui Town, Chongzuo City, Guangxi, and its detailed composition and properties are outlined in Table 4.

Table 4. P·O42.5 characteristics of ordinary Portland cement.

| Specific Surface Area (m ² /kg) | Loss on Ignition (%) | Setting Time (min) | | Stability | Compressive Strength (MPa) | | Bending Strength (MPa) | |
|--|----------------------|--------------------|---------------|-----------|----------------------------|------|------------------------|-----|
| | | Initial Setting | Final Setting | | 3d | 28d | 3d | 28d |
| ≥300 | ≤3.5 | ≥45 | ≤390 | Qualified | 24.8 | 48.9 | 5.0 | 8.1 |

2.1.5. Mineral Admixture

To enhance the mechanical properties of concrete, it is necessary to include mineral admixtures such as fly ash (FA) and silica fume (SF) with a purity of 95% [22]. These additives are obtained from the Dong Qiang Mineral Processing Factory in Lingshou County, Shijiazhuang City, Hebei Province. Refer to Table 5 for their basic properties.

Table 5. Technical properties of fly ash and silica fume.

| Flyash | | | | | | | |
|---------------------|-----------------------------------|----------------|------------------|-------------------------------|---------------------------|---------------------|--|
| Loss on Ignition/% | Water Demand Ratio/% | Moisture/% | Dissociate CaO/% | Screen Allowance of 0.45 mm/% | SO ₃ Content/% | | |
| 3.2 | 91 | 0.3 | 0.6 | 7.6 | 1.6 | | |
| Silica Fume | | | | | | | |
| SiO ₂ /% | Fe ₂ O ₃ /% | refractoriness | CaO/% | MgO/% | NaO/% | TiO ₂ /% | The passing rate of 200 mesh screens/% |
| 99.23 | 0.01 | 1760 °C | 0.01 | 0.01 | 0.05 | 0.03 | 95.2 |

2.1.6. Water-Reducing Agent

UHPC requires a significant amount of high-efficiency water-reducing agents to achieve optimal results. The polycarboxylic acid-based water-reducing agent [23] utilized in this study is manufactured by Hunan Zhongyan Building Materials Technology Co., Ltd. (Changsha, China) and boasts excellent water retention and an ultra-high water-reducing rate. The primary performance index for this agent can be found in Table 6 below.

Table 6. Performance indexes of polycarboxylic acid water-reducer.

| Number | Inspection Item | Unit | Standard Requirements | Test Result | Individual Evaluation |
|--------|----------------------|------|-----------------------|-------------|-----------------------|
| 1 | Water reduction rate | % | ≥25 | 27 | qualified |
| 2 | Bleeding rate ratio | % | ≤60 | 30 | qualified |

Table 6. Cont.

| Number | Inspection Item | | Unit | Standard Requirements | Test Result | Individual Evaluation |
|--------|------------------------------------|-----------------|------|-----------------------|-------------|-----------------------|
| 3 | Gas content | | % | ≤ 6.0 | 3.4 | qualified |
| 4 | The difference in coagulation time | Initial setting | min | $-90\sim+120$ | +28 | qualified |
| | | Final setting | min | $-90\sim+120$ | +34 | qualified |
| 5 | Time variation (slump) of 1 h | | mm | ≤ 80 | 40 | qualified |
| 6 | Compressive strength ratio | 1 d | % | ≥ 170 | 178 | qualified |
| | | 3 d | % | ≥ 160 | 167 | qualified |
| | | 7 d | % | ≥ 150 | 156 | qualified |
| | | 28 d | % | ≥ 140 | 147 | qualified |
| 7 | Shrinkage ratio | | % | ≤ 110 | 98 | qualified |

2.1.7. Fiber [24]

The appropriate utilization of fiber has dramatically improved the characteristics of concrete, mainly for UHPC-AC. To attain the desired strength, steel fiber (SF), polyvinyl alcohol fiber (PVA), and polypropylene fiber (PP) were employed in this study, and the physical properties of these three fibers are presented in Table 7.

Table 7. The physical properties of different fibers.

| Fiber Type | Diameter (mm) | Length (mm) | Density (kg/m ³) | Modulus of Elasticity (GPa) | Fracture Strength (MPa) | Tensile Elongation (%) |
|------------|---------------|-------------|------------------------------|-----------------------------|-------------------------|------------------------|
| SF | 0.2 | 12 | 7800 | 200 | 1130 | 1.8 |
| PVA | 0.02 | 12 | 970 | 85 | 3000 | 6.0 |
| PP | 0.02 | 12 | 920 | 110 | 3000 | 8.7 |

2.1.8. Detailed Information of Test Materials

Several photo samples of different materials were prepared for this experiment, as illustrated in Figure 2.

2.2. Detection Instrument

This experiment aims to test the compressive strength and appearance analysis of UHPC-CA. The following tools will be used:

1. A hammer crusher from Pioneer Instrument Co., Ltd. (Dalian, China) can screen aggregates with a particle size range of 150 mm to 10 mm.
2. A vibrating screen machine manufactured by Shanghai Xing Building Materials Test Equipment Co., Ltd. (Shanghai, China) with a shaking frequency of up to 221 times/minute and a motor power of 0.37 kW.
3. A constant temperature drying oven from Shanghai Luda Experimental Instrument Co., Ltd. with a size of 500 × 600 × 750 mm and a room temperature range of 10 °C to 300 °C.
4. An electronic scale manufactured by Shuang Jie Test Instrument Factory, Changshu, with a maximum range of 100 kg and an accuracy of 10 g.
5. A concrete mixer from the same manufacturer as the vibrating screen machine with a predetermined mixing capacity of 60 kg, a shaft speed of 47 rpm, and a rated power of 2.2 kW.
6. A vibrating table made by the same batch of Roots mixers with an overall size of 1000 mm × 1000 mm, a vibration frequency of 2860 times/min, and a maximum load-bearing capacity of 200 kg.

7. A curing box produced by Shanghai Luda Experimental Instrument and Equipment Co., Ltd. with a controlled temperature of 20 ± 1 °C, relative humidity of $\geq 90\%$, a heating power of 800 w, and a cooling capacity of 145 w.
8. A TYE-2000E pressure testing machine produced by Wuxi Jianyi Instrument Machinery Co., Ltd. (Wuxi, China), with a maximum pressure of 2000 kN.



(a) Granite macadam



(b) Oyster shell coarse aggregate



(c) Cone shells



(d) River Sand



(e) Sea sand

Fine aggregate



(f) Cement



(g) Fly ash powdered substance



(h) Silica fume



(i) SF



(j) PVA fibers



(k) PP

Figure 2. Detailed information on various test materials.

2.3. Setting of Mixing Ratio

The mixed proportion of this study was collected from relevant papers at home and abroad, and an orthogonal test was carried out in combination with the actual situation in the laboratory [25]. The mixed proportion scheme is shown in Table 8.

Table 8. UHPC-CA mix proportion (kg/m³).

| Number | Coarse Aggregate | Fine Aggregate | Cement | Silica Fume | Flyash | Water | Water-Reducing | Fibre |
|--------|------------------|----------------|--------|-------------|--------|---------|----------------|-------|
| 1 | 500 (S) | 1006 (W) | 660 | 83 | 83 | 132 (W) | 43 | SF |
| 2 | 500 (S) | 1006 (W) | 660 | 83 | 83 | 132 (W) | 43 | PVA |
| 3 | 500 (S) | 1006 (W) | 660 | 83 | 83 | 132 (W) | 43 | PP |
| 4 | 500 (S) | 1006 (S) | 660 | 83 | 83 | 132 (S) | 43 | SF |
| 5 | 500 (O) | 1006 (S) | 660 | 83 | 83 | 132 (S) | 43 | SF |
| 6 | 500 (C) | 1006 (S) | 660 | 83 | 83 | 132 (S) | 43 | SF |

Note: Based on the results of this experiment, it was found that the compressive strength of steel fiber in UHPC-CA is satisfactory. Therefore, steel fiber will be added to the mix for the remaining experiments. The table includes abbreviations for coarse and fine aggregates and mixing water. S stands for crushed stone, O represents oyster shell, and C represents cone shell. W and S stand for river sand and sea sand, respectively, while W and S in mixed water indicate fresh water and seawater, respectively.

The main variables being tested are the type and amount of coarse and fine aggregates, mixing water, and mixed fiber. To aid in understanding, we have provided Table 9 below.

Table 9. Distribution of mixture ratio variables of UHPC-CA.

| Number | Coarse Aggregate | Fine Aggregate | Mixing Water | Fibre |
|--------|------------------|----------------|--------------|-------------------|
| 0 | Stone | Sea sand | Sea water | 0% |
| 1 | Stone | River sand | Freshwater | 0% |
| 2 | Stone | River sand | Freshwater | 1.5% SF |
| 3 | Stone | River sand | Freshwater | 1.5% PVA |
| 4 | Stone | River sand | Freshwater | 1.5% PP |
| 5 | Stone | River sand | Freshwater | 2% SF |
| 6 | Stone | River sand | Freshwater | 2% PP |
| 7 | Stone | River sand | Freshwater | 1.5% SF + 0.5 PVA |
| 8 | Oyster (I) | Sea sand | Sea water | 0% |
| 9 | Oyster (II) | Sea sand | Sea water | 0% |
| 10 | Oyster (I) | Sea sand | Sea water | 1.5% SF |
| 11 | Oyster (I) | Sea sand | Sea water | 1.5% SF + 0.5 PVA |
| 12 | Cone | Sea sand | Sea water | 0% |
| 13 | Cone | Sea sand | Sea water | 1.5% SF |
| 14 | Cone | Sea sand | Sea water | 1.5% SF + 0.5 PVA |

Note: The term “stone” pertains to rubble made from granite. “Oyster” refers to the use of oyster shells as an aggregate, with “Oyster I” indicating oyster shell particles ranging in size from 4.75 to 15 mm, and “Oyster II” referring to oyster shell particles ranging from 9.5 to 15 mm in size. “Cone” refers to collecting shells from this type of cone shells. “SF” stands for steel fiber, “PVA” denotes polyvinyl alcohol fiber, and “PP” represents polypropylene fiber.

3. Testing Process

3.1. Compression Strength Test

Based on the guidelines in SL 352-2006 (2006) [26], the compressive strength test requires a sample size of a non-standard 100 × 100 × 100 mm cube. For each stage, three samples are taken from each group, divided into 3, 7, and 28 days. There are 15 groups, with a combined total of 135 pieces. As per the code, the loading rate of concrete blocks above grade C80 should be between 0.8 and 1.0 MPa/s. This study utilized a pressure testing machine with a maximum test force of 2000 kN and a loading rate of 0.8 MPa/s. The experimental value of compressive strength should be adjusted by multiplying it with a conversion factor of 0.95, which will provide the final strength value.

3.2. Detection Process

To create a concrete block, follow these steps:

1. Collect the necessary materials, including shells, sea sand, and seawater test materials.
2. Clean the shells and remove impurities from the sea sand. Using a vibrating screen, separate sand particles with a size of 0.15–4.75 mm. Seawater can be used without treatment.
3. Place an appropriate amount of fine aggregate, cement, and mineral powder into a dryer to dry.
4. Weigh the processed materials in proportion for later use.
5. Coat the inner surface of a $100 \times 100 \times 100$ mm trihedral die with a release agent.
6. Mix the coarse and fine aggregates in a blender for 1 min. Add cement and stir for 1 min.
7. Mix the water reducer in the mixing water, then slowly pour 2/3 of the solution while stirring and add the remaining 1/3.
8. Sprinkle fibers into the concrete within 5 min.
9. Pour the concrete into a tray and conduct slump and expansion tests.
10. Fill the die twice, compacting the first half with iron bars, and repeat on the second half.
11. Vibrate the concrete on a vibrating table for 30 s to remove bubbles and excess concrete.
12. Scrape the surface of the test block with a scraper and control excess parts within 1 mm of the die.
13. Mark the specimen and affix a plastic film to prevent water loss.
14. After 48 h, de-mold the block and cure it in a standard curing box at a temperature of 70 ± 2 °C and humidity of not less than 95%.
15. On the 3rd, 7th, and 28th day, remove the block, dry the surface, and test its compressive strength with an instrument. Record the data.

The production process meets the required specifications [27], and the drawing test process is illustrated in Figure 3.

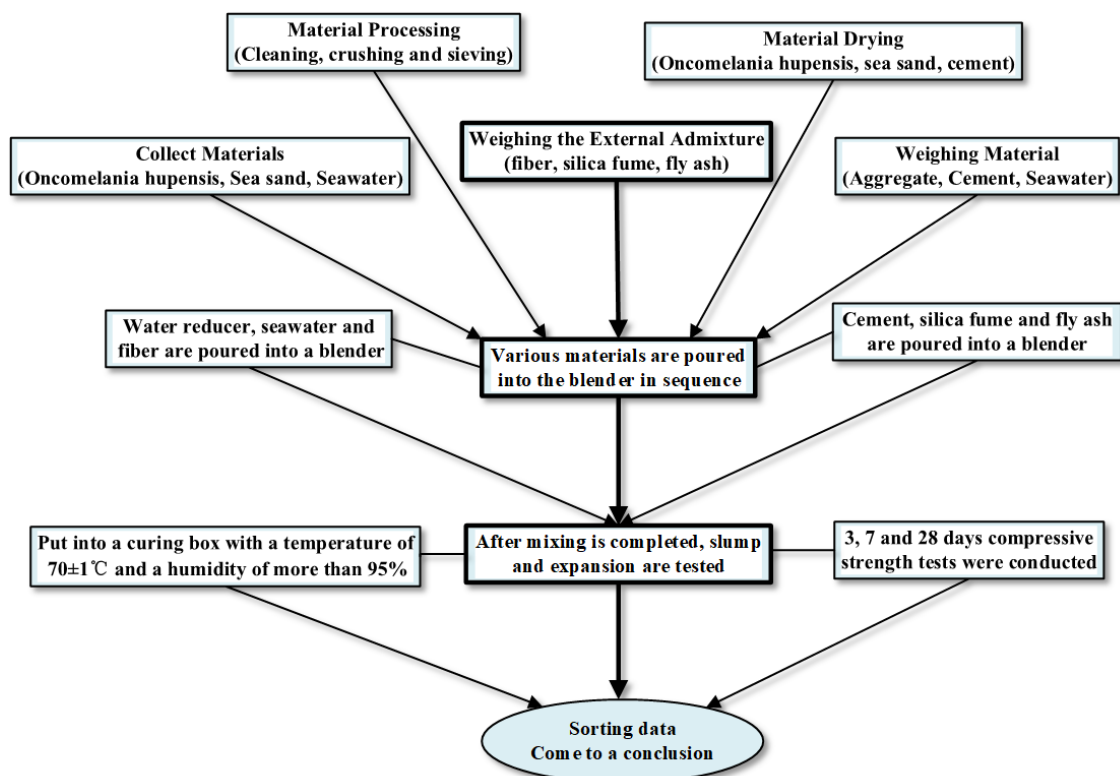


Figure 3. Marine UHPC-SCA test flow.

4. Analysis and Discussion of Data

4.1. Flow Properties of UHPC-SCA

4.1.1. Measurement Steps

The fluidity of concrete work is an important indicator that directly affects construction efficiency [28]. In this study, hydrophilic materials such as polyethylene fiber, polypropylene fiber, and steel fiber were used. Their water absorption may affect the overall compactness of marine UHPC-CA. Therefore, it is necessary to determine the influence of various factors on the working performance of UHPC-CA. The evaluation standard for working performance is based on the influence of different volume content of three kinds of fibers on slump and swelling degree. The test is conducted per the Standard of Test Methods for Performance of Ordinary Concrete Mixtures (GB/T 50080-2016) [29]. The working performance of cement mortar is evaluated by slump and slump expansion. The testing steps are as follows:

- (1) Firstly, thoroughly wet the slump cone, funnel, and measuring tool. Then, place the funnel above the slump cone;
- (2) Put the cement mortar into the slump cone three times equally and tamp it with a vibrating rod 20 times after each loading. This ensures the uniform distribution of the cannon on the cross-section. Clean up the excess concrete after loading and finally smooth the top surface;
- (3) Lift the cylinder vertically and smoothly, measure its slump and expansion after 60 s, and control the entire process within 3 min.

4.1.2. Data Analysis

The slump and swelling data of each group of marine UHPC-CA obtained from experimental measurement are integrated, as shown in Table 10.

Table 10. Flow performance of marine UHPC-CA in each group.

| Number | Coarse Aggregate | Fiber | Slump /mm | Expansion /mm |
|--------|------------------|-------------------|-----------|---------------|
| 0 | Gs | 0% | 285 | 490 |
| 1 | G | 0% | 290 | 500 |
| 2 | G | 1.5% SF | 280 | 490 |
| 3 | G | 1.5% PVA | 90 | 300 |
| 4 | G | 1.5% PP | 85 | 290 |
| 5 | G | 2% SF | 230 | 460 |
| 6 | G | 2% PP | 30 | 230 |
| 7 | G | 1.5% SF + 0.5 PVA | 155 | 320 |
| 8 | OI | 0% | 220 | 450 |
| 9 | OII | 0% | 215 | 440 |
| 10 | OI | 1.5% SF | 190 | 360 |
| 11 | OI | 1.5% SF + 0.5 PVA | 150 | 320 |
| 12 | C | 0% | 260 | 470 |
| 13 | C | 1.5% SF | 210 | 440 |
| 14 | C | 1.5% SF + 0.5 PVA | 160 | 340 |

Note: The table provided shows the abbreviations for various materials used in the study. G represents granite gravel, Gs represents granite seawater sand, O represents oyster shell, and C represents cone shell. SF is an abbreviation for steel fiber, PVA refers to polyvinyl alcohol fiber, and PP stands for polypropylene fiber.

Table 10 indicates that UHPC-CA made from granite has a fluidity that is only slightly different from that of sea sand or freshwater river sand, with a difference of only about 2%. This means that in situations in which laboratory materials are limited, granite, fresh water, and river sand can be used as controls to initially configure UHPC-SCA with better performance.

Additionally, as shown in Figure 4, SF, PVA, and PP impact the fluidity of concrete, but they all have a restraining effect [30].

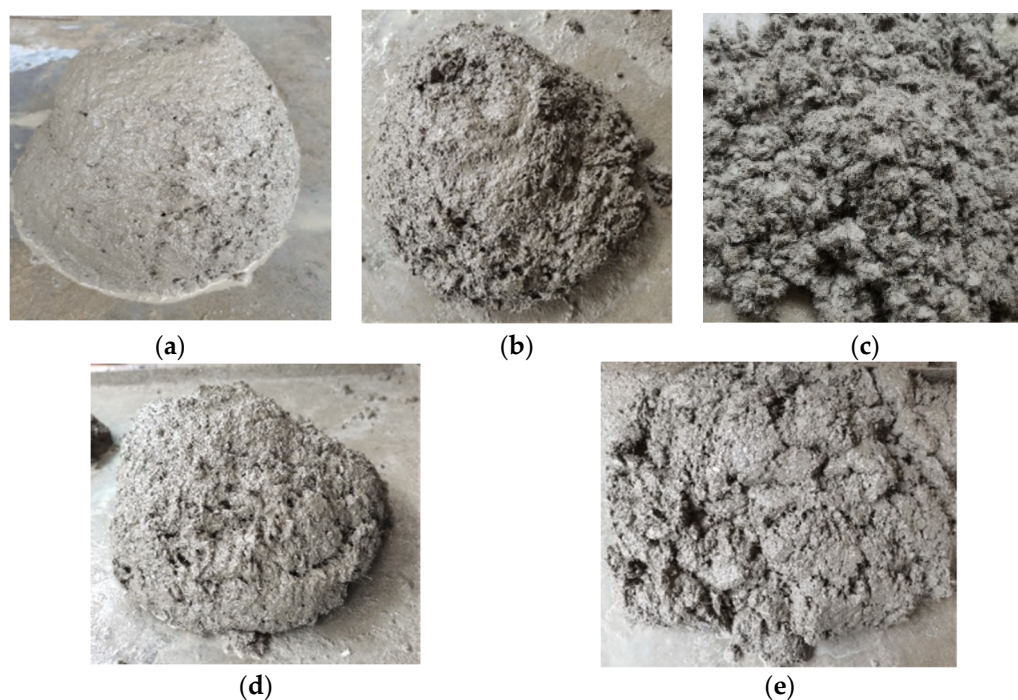


Figure 4. Effect of different fibers and aggregates on the fluidity of UHPC-CA. (a) SF, (b) PVA, (c) PP, (d) oyster shell, (e) cone shell.

1. Based on the information presented in Figure 5a, the consistency and expansion level of UHPC-CA seashells differ depending on the type of coarse aggregate used. Out of the options tested, ordinary granite gravel performed the best, followed by oniomania shell. Oyster shells, on the other hand, showed relatively poor fluidity. The percentages of the latter two were 89.7% to 94% and 75.9% to 90% of the former, respectively, corresponding to the water absorption rates of the various coarse aggregates shown above.

2. In Figure 5b, the changes in the fluidity of three types of fibers and their amounts in ordinary granite UHPC-CA are depicted. The figure reveals that adding fiber results in the best slump and expansion rates for UHPC-CA. When the content of these three fibers is at 1.5%, SF has a minimal effect on fluidity, only about 2% to 3%. In contrast, PVA and PP significantly impact fluidity, ranging from 40% to 70%, mainly due to the influence of fiber manufacturing materials. As the fiber content increased from 1.5% to 2%, the slump and expansion rate of UHPC-CA decreased slightly. Specifically, PP's slump and expansion rate decreased by 64.7% and 20.7%, respectively, while the two fluidity indicators of SF decreased by 17.9% and 6.1%, respectively. Furthermore, the fluidity of UHPC-CA with 1.5% SF and 0.5% PVA falls between 2% SF and 2% PP.

3. When using cone shell as a coarse aggregate without fiber in granite macadam, it has the most significant slump and swelling degree. However, adding SF reduces these effects. Adding two kinds of fibers significantly reduces fluidity. This principle also applies to oyster shells, as shown in Figure 5d. Choosing the appropriate proportion of external fibers to optimize fluidity is essential.

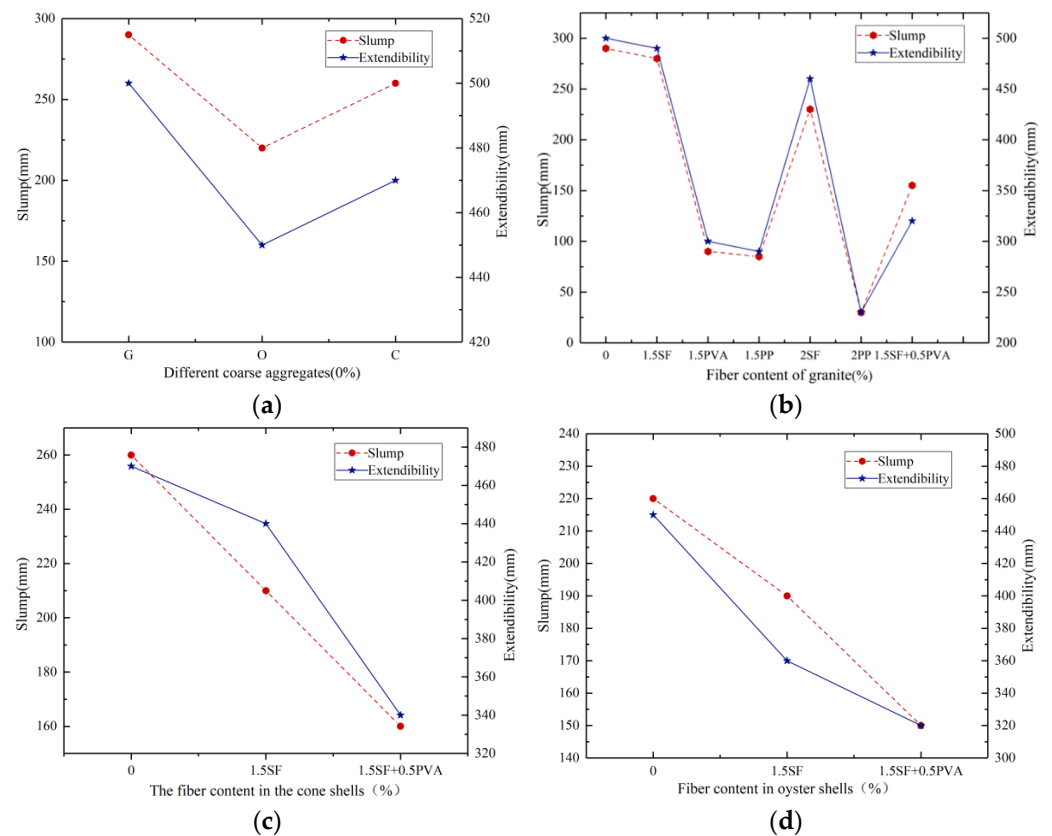


Figure 5. Comparison of slump and spread of UHPC-CA in each group. (a) Different coarse aggregates, (b) Fiber content of granite, (c) The fiber content in the cone shells, (d) The fiber content in the Oyster shells.

4.2. Analysis of Compressive Strength

For this research, we utilized the maximum compression force recorded by the pressure-testing device. We then computed this value based on the guidelines outlined in the Test Method for Physical and Mechanical Properties of Concrete (GB/T 50081—2019) [31]. Please refer to Formula (1) for the specific formula used for calculation.

$$f_{cu} = \gamma \frac{F}{A} \quad (1)$$

Formula: f_{cu} —the compressive strength of concrete cube specimens (MPa);

γ —the empirical coefficient is 0.95;

F —specimen failure load (kN);

A —pressure bearing area of the specimen (mm^2).

To account for any accidental errors in the experiment, it is recommended that we take three samples as a group. The maximum and minimum values should not differ by more than 15% from the median [32]. Finally, we can calculate the average value using Formula (2).

$$f_{cc} = \frac{f_{cu1} + f_{cu2} + f_{cu3}}{3} \quad (2)$$

Formula: f_{cc} —the average compressive strength of concrete cube specimens (MPa).

4.2.1. An Analysis of the Adaptability of Crushed Granite Stone

Table 11 displays that the compressive strength of G0 and G1 undergoes a 1% change from 3 days to 28 days. This is achieved by using granite crushed stones with a particle size of 4.75–9.5 mm as coarse aggregate and incorporating different mixed water and fine

aggregate without fiber. The compressive properties of other samples of various marine aggregates are also analyzed.

Table 11. Peak load and compressive strength of UHPC-CA marine shells.

| No | 3d | | | | 7d | | | | 28d | | | |
|-----|-------|-----|---------------|------|-------|------|---------------|------|-------|------|---------------|-------|
| | F /kN | | f_{cc} /MPa | | F /kN | | f_{cc} /MPa | | F /kN | | f_{cc} /MPa | |
| G0 | 650 | 656 | 635 | 61.4 | 804 | 798 | 785 | 75.6 | 880 | 892 | 891 | 84.3 |
| G1 | 706 | 634 | 633 | 62.5 | 780 | 797 | 802 | 75.3 | 878 | 901 | 860 | 83.6 |
| G2 | 728 | 878 | 822 | 76.9 | 924 | 1011 | 1129 | 97.1 | 1133 | 1140 | 1126 | 107.5 |
| G3 | 659 | 724 | 661 | 64.7 | 780 | 761 | 738 | 72.3 | 890 | 886 | 878 | 84.1 |
| G4 | 678 | 622 | 702 | 63.4 | 825 | 836 | 804 | 78.4 | 918 | 900 | 929 | 87.3 |
| G5 | 749 | 710 | 733 | 69.4 | 889 | 878 | 866 | 83.2 | 1028 | 966 | 975 | 94.0 |
| G6 | 575 | 541 | 568 | 53.3 | 624 | 632 | 636 | 59.9 | 713 | 711 | 713 | 67.7 |
| G7 | 569 | 540 | 591 | 54.2 | 756 | 791 | 825 | 75.1 | 991 | 957 | 955 | 91.9 |
| O8 | 463 | 510 | 460 | 45.4 | 517 | 592 | 549 | 52.5 | 579 | 582 | 590 | 55.5 |
| O9 | 567 | 544 | 548 | 52.8 | 592 | 549 | 568 | 54.6 | 590 | 600 | 596 | 56.9 |
| O0 | 652 | 578 | 569 | 57.0 | 738 | 757 | 706 | 69.7 | 820 | 750 | 750 | 73.5 |
| O11 | 533 | 518 | 515 | 49.4 | 568 | 592 | 600 | 55.9 | 584 | 636 | 647 | 59.1 |
| C12 | 649 | 639 | 657 | 61.1 | 764 | 670 | 706 | 67.8 | 903 | 952 | 924 | 88.0 |
| C13 | 824 | 922 | 850 | 82.3 | 997 | 1015 | 1087 | 98.1 | 1146 | 1099 | 1121 | 106.6 |
| C14 | 477 | 533 | 549 | 60.6 | 725 | 765 | 712 | 69.7 | 817 | 789 | 816 | 77 |

1. In Figure 6a, during the three stages, there is a slight fluctuation in the error of the 28-day compressive strength, but there is a significant fluctuation in the 7-day strength. A comparison is made between the compressive strength of granite crushed stone with three types of fibers and varying amounts of content. It was observed that different fibers and content levels have varying effects on UHPC-CA. Firstly, the compressive strength of UHPC-CA and fibers was enhanced, with SF showing better results than PVA [33]. Secondly, the mixing effect could have been more effective than a single fiber.

2. Looking at Figure 6b, it is clear that the error of G2 for three and seven days fluctuates wildly when the SF content changes from 0 to 2%. At a content of 1.5%, the 28-day strength reaches 107.5 MPa, whereas the range is only 94 MPa for 2%, resulting in a 15% difference. However, this is still a significant improvement for those without fiber, with 28.6% and 12.4% optimization rates, respectively. Furthermore, the 28-day compressive strength of concrete blocks mixed with 1.5% SF and 0.5% PVA is only 91.9 MPa, which is not as good as that of concrete blocks combined with 1.5–2% SF.

3. Figure 6c compares adding SF, PVA, and PP into granite UHPC-CA. The mixing amount of them is 1.5%. As can be seen from the figure, the order of action of the three kinds of fibers on concrete is as follows: SF > PP > PVA. Of course, compared with pure UHPC-CA, the compressive strength of these samples has improved, increasing by 28.6%, 4.43%, and 0.6%, respectively.

4. In Figure 6d, the total fiber content is 2%, from which it is found that excessive use of SF and PP will reduce the compressive strength of UHPC-CA, and the most severe thing is that the performance of the specimen doped with PP is lower than that of the sample doped with 1.5% by more than 20%.

The analysis of the compressive properties of UHPC-CA granite crushed stone shows that the best fiber type is SF and that the best fiber content is 1.5% of single content.

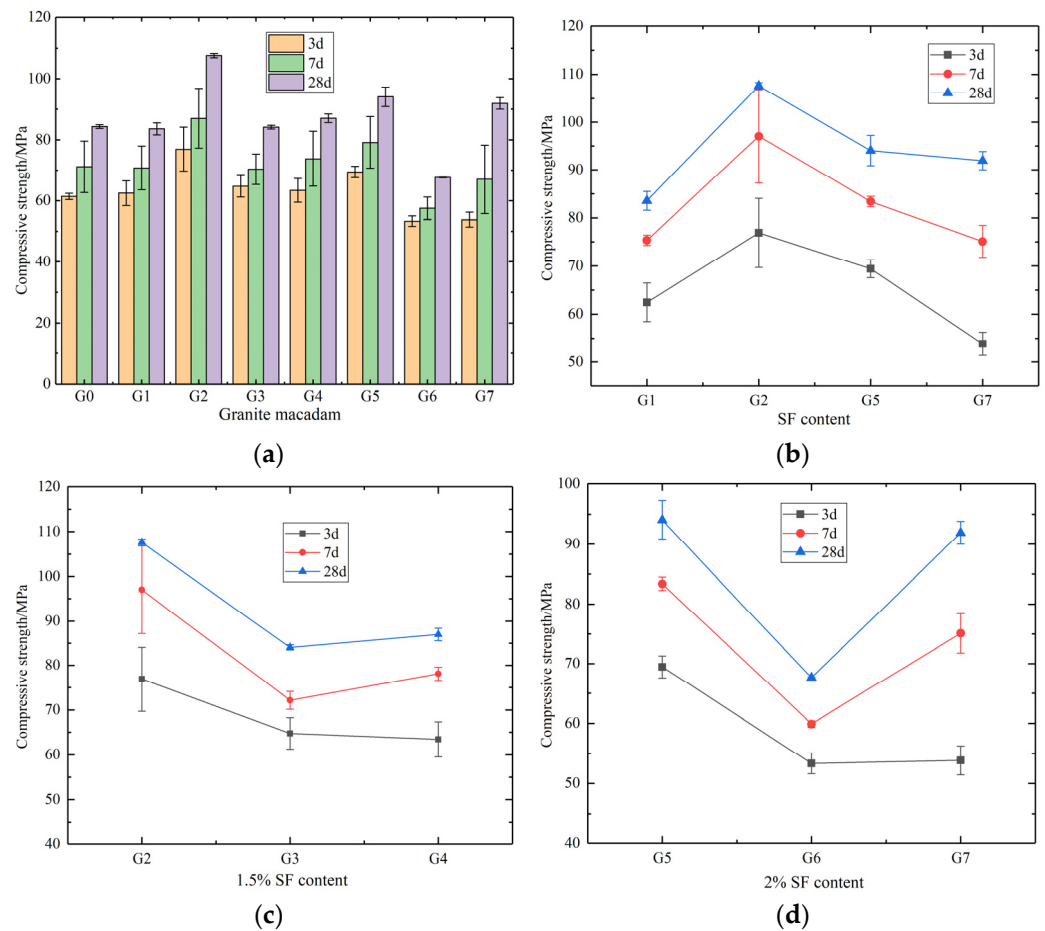


Figure 6. Compressive strength of granite UHPC-CA. (a) Granite macadam, (b) SF content, (c) 1.5% SF content, (d) 2% SF content.

4.2.2. UHPC-CA Analysis of Oyster Shells

According to UHPC-CA, made of granite gravel, adding 1.5% SF to concrete can effectively improve the compressive strength of the specimen.

1. Based on the data presented in Figure 7a, the compressive strength of UHPC is highest when oyster shells with particle sizes of 4.75~9.5 mm, 9.5~15 mm, and 9.5~15 mm are used as coarse aggregate. This strength is most prominent within the first three days after preparation. However, the strength continues to increase from 7 to 28 days, reaching about 55 MPa. It is important to note that the strength of the oyster shell aggregate has reached its maximum potential and cannot be improved regardless of the water–cement ratio used.

2. According to the data presented in Figure 7b, the fluctuation of compressive strength of O10 is higher than that of the other two groups. The internal density of UHPC-SCA is altered when 1.5% SF is introduced. This change results in a specimen strength of approximately 60 MPa after three days. After 28 days of curing, the strength of the specimen increases significantly, reaching 132% of the strength without adding fiber. While it may not fully meet the minimum standards for UHPC, the compressive strength has been sufficiently improved.

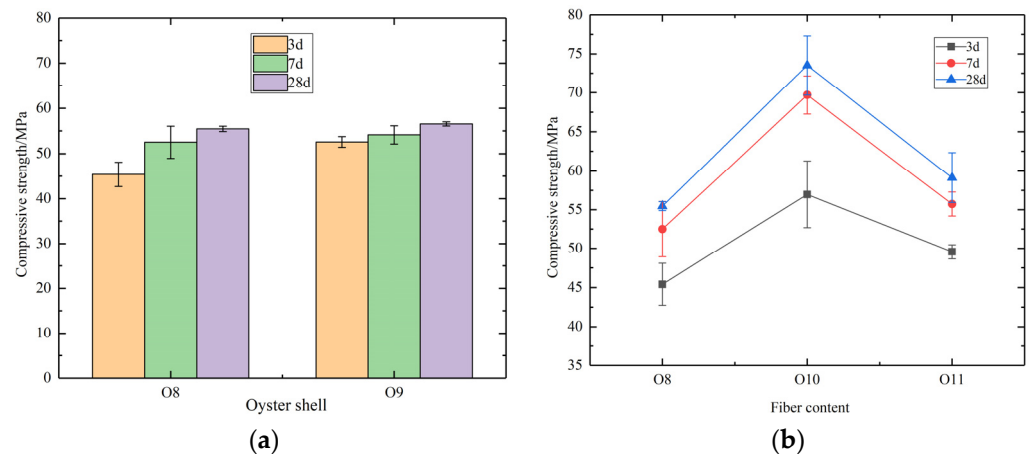


Figure 7. Compressive strength of oyster shells UHPC-SCA. (a) Oyster shell, (b) Fiber content.

4.2.3. The UHPC-SCA Analyzed Cone Shells

Coarse aggregates for UHPC-SCA are prepared from cone shells with a particle size of 4.75–9.5 mm. These shells are cleaned, dried, crushed, and powder-screened before use. Unlike oyster shell particles with a flaky distribution, cone shells are irregular, similar to granite. However, this irregularity can affect the performance of UHPC-SCA. Despite this, overall performance is comparable to ordinary granite.

Figure 8a shows that the compressive strength of UHPC-SCA mixed with SF and PVA is inferior to that without fiber. The difference in strength is 12.5% at 28 d. However, the compressive strength of the specimen mixed with 1.5% SF is comparable to that of ordinary granite gravel. Additionally, in Figure 8b, it is seen that the compressive properties of cone shells grow at a rate of 5.4% faster than granite at the age of 3d. Furthermore, the compressive strengths at 7 d and 28 d exceed 100 MPa. In Figure 8, it can be observed that the variation in error for UHPC-SCA with cone snail shells as coarse aggregate is comparatively less than that of UHPC-CA with granite aggregate.

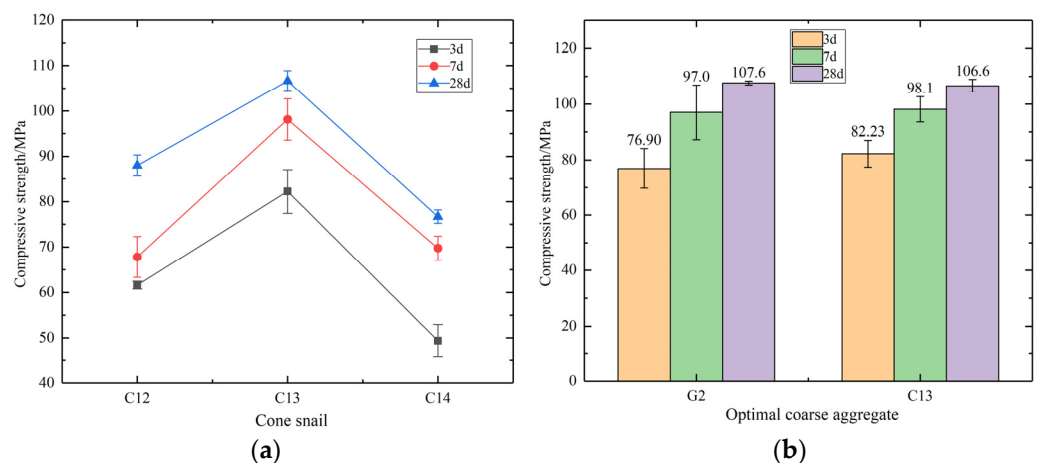


Figure 8. Compressive strength of cone shells UHPC-SCA. (a) Cone snail, (b) Optimal coarse aggregate.

4.3. Discussion on Marine UHPC-SCA Test

Generally, the fluidity of concrete is determined by its mechanical properties. In Figure 9, the fluidity value and compressive strength of UHPC-SCA are presented on the same chart for easy observation.

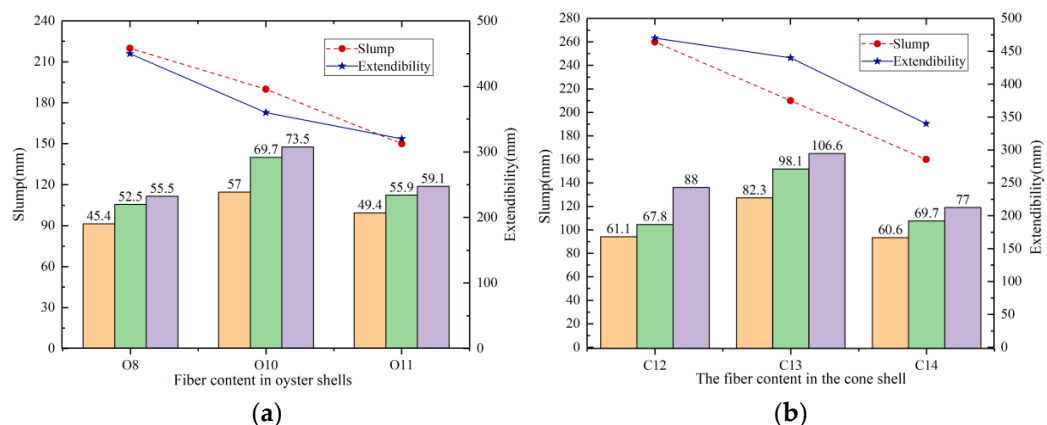


Figure 9. Relationship between fluidity and compressive strength of UHPC-CA in marine shells, seawater, and sea sand. (a) The fiber content in oyster shells, (b) The fiber content in the cone shells. Note: The diagram indicates the flow performance by the dotted line. The histogram shows the compressive strength, with orange representing 3 days, green representing 7 days, and purple representing 28 days.

It can be found from Figure 9 that the slump and expansion of UHPC-CA made of sea shells as coarse aggregate, sea sand as fine aggregate, and seawater are too high or too low, and their compressive strength is not as good as the performance between them. Additionally, its compressive strength could be better than the other options. The fluidity of the mixture is mainly affected by the amount of fiber added. It is essential to monitor the fluidity when adding fiber. The best compressive strength is achieved when the slump is within the range of 200–250 mm and the expansion is between 400–450 mm.

5. Conclusions

This paper investigates the coarse and fine aggregate, mixing water, fiber type, and content of UHPC-SCA. The test data provides comprehensive results.

1. The fluidity of concrete is affected by certain factors, such as SF, PVA, and PP. These components can limit the fluidity of concrete. When the content of these components is at 1.5%, the fluidity is ranked as SF > PVA > PP. With the addition of 2%, the fluidity ranking is SF > SF + PVA > PP.

2. By adding SF, the performance of UHPC-SCA is most improved when the water–cement ratio is 0.16, with an optimal dosage of 1.5%. UHPC-SCA, made of 4.75–9.5 mm cone shells, has a strength of 106 MPa, similar to that of ordinary granite gravel. UHPC-SCA made of oyster shells may have a better effect, but the maximum strength achieved is only 73 MPa.

3. The fluidity of marine UHPC-SCA is related to its bare mechanical properties. Its slump and expansion are too high or too low, and the best range is 200–250 mm slump and 400–450 mm expansion.

4. The experiment presents several challenges that need to be addressed. Specifically, we need to focus on removing bubbles in UHPC-SCA, finding the most effective way to distribute mineral powder and cement, and studying the impact of other types of fibers. These are all areas that require further investigation.

5. During this test, the following shortcomings were identified.

The test has a water–cement ratio of 0.16, meaning a significant amount of cement is used. Mixing concrete involves inhaling air and forming internal bubbles [34]. These bubbles can negatively impact the mechanical properties of the specimen, which is not ideal for studying UHPC-SCA. While the outer part of an oyster shell is the hardest, crushing it significantly reduces its strength. When preparing aggregate using UHPC-SCA, the resulting shape may need to be sturdier, which is unsuitable for studying marine concrete with good strength. Furthermore, a comparison of SF, PVA, and PP fibers revealed that SF lacks corrosion resistance and has limited application in coastal areas. Developing a

new type of fiber to replace steel fiber is necessary. The macroscopic images of various UHPC-CA test blocks in Figure 10 highlight the issues above.

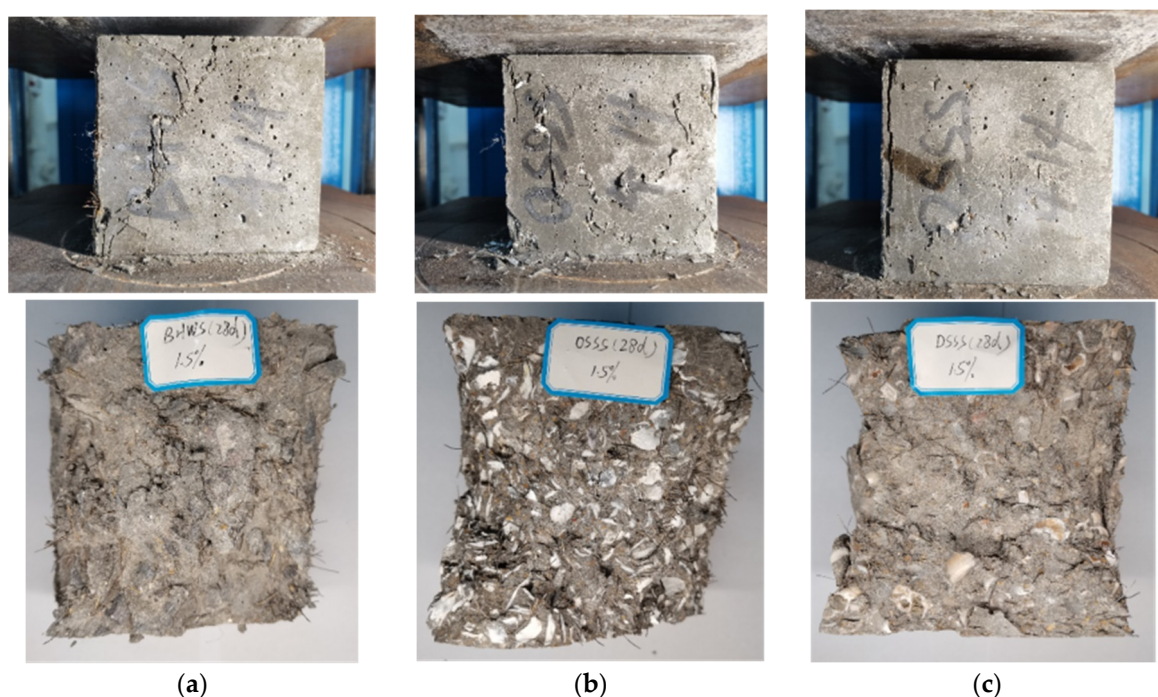


Figure 10. Macroscopic images of various UHPC-CA test blocks. (a) Granite macadam, (b) oyster shells, (c) cone shells.

Author Contributions: Conceptualization, S.W.; methodology and validation M.Z.; software, Y.S.; validation, L.C.; investigation, Y.Z. All authors have read and agreed to the published version of the manuscript.

Funding: This research was funded by the Guangxi Key Laboratory of Ocean Engineering Equipment and Technology, Qinzhou 535011, the China and Key Laboratory of Beibu Gulf Offshore Engineering Equipment and Technology (Beibu Gulf University), and the Education Department of Guangxi Zhuang Autonomous Region, Qinzhou 535011, China.

Data Availability Statement: Data are contained within the article.

Conflicts of Interest: The authors declare no conflict of interest.

References

1. Abdal, S.; Mansour, W.; Agwa, I.; Nasr, M.; Abadel, A.; Onuralp Özkılıç, Y.; Akeed, M.H. Development status and engineering application of ultra-high performance concrete. *Guangdong Civ. Archit.* **2022**, *29*, 90–92.
2. Huang, Z.; Shen, P. Experimental study on 200MPa ultra-high strength steel fiber concrete. *Concrete* **1993**, *3*, 5.
3. Chen, F.; Xu, F.; Zhang, G.; Ding, S.; Ming, Y. Study on fundamental properties of ultra-high performance concrete with coarse aggregate. In Proceedings of the 2018 National Academic Annual Meeting of Industrial Architecture, Beijing, China, 8 April 2018.
4. Long, K.; Sun, J.; Gao, J.; Sun, M.; Zhu, Y. Study on mechanical properties of polyethylene ultra-high performance concrete with coarse aggregate. *Value Eng.* **2023**, *42*, 130–133.
5. Liu, J.; Han, F.; Cui, G.; Zhang, Q.; Lv, J.; Zhang, L.; Yang, Z. The combined effect of coarse aggregate and fiber on tensile behavior of ultra-high performance concrete. *Constr. Build. Mater.* **2016**, *121*, 310–318. [[CrossRef](#)]
6. Kim, H.; Hadl, P.; Nguyen, V.T. A New mix design method for UHPC based on stepwise optimization of particle packing density. In Proceedings of the International Interactive Symposium on Ultra-High Performance Concrete, Des Moines, IA, USA, 18–20 July 2016; Iowa State University Digital Press: Ames, IA, USA, 2016; Volume 1.
7. Li, S.; Jensen, O.M.; Wang, Z.; Yu, Q. Influence of micromechanical property on the rate-dependent flexural strength of ultra-high performance concrete containing coarse aggregates (UHPC-CA). *Compos. Part B Eng.* **2021**, *227*, 109394. [[CrossRef](#)]
8. Peng, G.; Yang, J.; Gao, Y.; Wang, B. Influencing factors of compressive strength of ultra-high performance concrete with coarse aggregate. *J. North China Inst. Water Resour. Hydropower* **2012**, *33*, 5–9.

9. Huang, Y.; Yu, Z. Experimental study of the bonding behavior between coarse aggregate ultra-high performance concrete and steel rebar. *Eng. Struct.* **2023**, *288*, 116253. [[CrossRef](#)]
10. Zhengyu, H.; Shigen, L. Study on mechanical properties of ultra-high performance concrete with coarse aggregate. *J. Hunan Univ.* **2018**, *45*, 47–54.
11. Yang, F.; Bank, J.; Wei, L.; Chang, Z.; Da, F. Experimental study on ultra-high performance concrete with coarse aggregate. *Concrete* **2018**, *12*, 110–113.
12. Zhang, X. Influence of coarse aggregate size and content on performance of ultra-high performance concrete. *Concr. World* **2023**, *1*, 17–22.
13. Li, S.; Zheng, W.; Zhou, W.; Wang, Y. Local compression capacity of ultra-high performance concrete containing coarse aggregate: Testing and calculation method. *J. Build. Eng.* **2023**, *76*, 107411. [[CrossRef](#)]
14. Zheng, X.; Chen, X.; Yue, Z.; Yao, F. Promotion, Opportunities, and Challenges of Marine Sustainable Development in China. *Environ. Pollut. Prev.* **2021**, *43*, 521–526.
15. Martínez-García, C.; González-Fontebo, B.; Martínez-Abella, F.; Carro-López, D. Performance of mussel shell as aggregate in plain concrete. *Constr. Build. Mater.* **2017**, *139*, 570–583. [[CrossRef](#)]
16. Khankhaje, E.; Salim, M.R.; Mirza, J.; Salmiati; Hussin, M.W.; Khan, R.; Rafieizonooz, M. Properties of quiet pervious concrete containing oil palm kernel shell and cockleshell. *Appl. Acoust.* **2017**, *122*, 113–120. [[CrossRef](#)]
17. Zheng, X.; Ling, B.; Huang, H.; Hai, Y. Experimental study on the influence of snail sand replacement rate on the mechanical properties of mortar in Nanhai. *Concrete* **2022**, *12*, 91–95.
18. Alidoust, P.; Goodarzi, S.; Amlashi, A.T.; Sadowski, Ł. Comparative analysis of soft computing techniques in predicting seashell-containing concrete's compressive and tensile strength. *Eur. J. Environ. Civ. Eng.* **2023**, *27*, 1853–1875. [[CrossRef](#)]
19. Bellei, P.; Torres, I.; Solstad, R.; Flores-Colen, I. Potential Use of Oyster Shell Waste in the Composition of Construction Composites: A Review. *Buildings* **2023**, *13*, 1546. [[CrossRef](#)]
20. Mo, K.H.; Alengaram, U.J.; Jumaat, M.Z.; Lee, S.C.; Goh, W.I.; Yuen, C.W. Recycling of seashell waste in concrete: A review. *Constr. Build. Mater.* **2018**, *162*, 751–764. [[CrossRef](#)]
21. Wen, C. Study on preparation and performance of environment-friendly coarse aggregate ultra-high performance concrete. *Munic. Technol.* **2023**, *41*, 35–39.
22. Liu, J.; Shi, C.; Wu, Z. Hardening, microstructure, and shrinkage development of UHPC: A review. *J. Asian Concr. Fed.* **2019**, *5*, 1–19. [[CrossRef](#)]
23. Jin, H.; Gong, Y.; Jiang, L.; Cheng, G. Development status of polycarboxylic acid superplasticizer for concrete. *Tianjin Chem. Ind.* **2018**, *32*, 4–5.
24. Chen, B.; Lin, Y.; Yang, J.; Huang, Q.; Huang, W.; Yu, X. Summary of fiber function in ultra-high performance fiber reinforced concrete. *J. Fuzhou Univ.* **2020**, *48*, 58–68.
25. Zhao, W.S.; Chen, W.Z.; Tan, X.J.; Huang, S. Study on foamed concrete used as seismic isolation material for tunnels in rock. *Mater. Res. Innov.* **2013**, *17*, 465–472. [[CrossRef](#)]
26. Nanjing Hydraulic Research Institute. *Hydraulic Concrete Test Procedures*; China Electric Power Press: Beijing, China, 2002.
27. Qiu, Z.; Liu, R.; Xiong, Z. Research progress in preparation and engineering application of UHPC ultra-high performance concrete. *Guangdong Archit. Civ. Eng.* **2023**, *2*, 30.
28. Quan, J.Z.J. Study on fluidity and mechanical properties of ecological ultra-high performance concrete mixed with coarse aggregate. *Jiangxi Build. Mater.* **2008**, *4*, 3–7.
29. CN-GB; The Standard for Performance Test Method of Ordinary Concrete Mixture. Domestic-National Standard-State Administration of Market Supervision. China Building Industry Press: Beijing, China, 2003.
30. Qi, J.; Dai, L.; Chai, T.; Chen, H.; Luo, Z. Influence of PVA fiber on properties of ultra-high performance concrete. *Jiangxi Build. Mater.* **2022**, *12*, 27–28.
31. GB/T 50081-2019; Standard for Test Methods of Physical and Mechanical Properties of Concrete. China Building Industry Press: Beijing, China, 2019.
32. AQSIQ; Concrete Strength Inspection and Evaluation Standard. China Institute of Building Science: Beijing, China; Construction Engineering Group Co., Ltd.: Beijing, China; Hunan University: Changsha, China, 2010.
33. Su, J.; Li, L.; Wu, P. Study the influence of steel and PVA fiber on the strength and abrasion resistance of ultra-high performance concrete. *Concr. Cem. Prod.* **2019**, *11*, 39–42.
34. Chong, W.; Pu, X.; Chen, K.; Liu, F.; Wu, J.; Peng, X. Hydration process test of ultra-low water-binder ratio cement paste materials. *J. Mater. Sci. Eng.* **2008**, *26*, 852–857.

Disclaimer/Publisher's Note: The statements, opinions and data contained in all publications are solely those of the individual author(s) and contributor(s) and not of MDPI and/or the editor(s). MDPI and/or the editor(s) disclaim responsibility for any injury to people or property resulting from any ideas, methods, instructions or products referred to in the content.